



ARL-TR-7718 • JULY 2016



Microelectromechanical System (MEMS) Gyroscope Noise Analysis and Scale Factor Characterization over Temperature Variation

by Angela Maio, Ryan Knight, and William Nothwang

Approved for public release; distribution is unlimited.

NOTICES

Disclaimers

The findings in this report are not to be construed as an official Department of the Army position unless so designated by other authorized documents.

Citation of manufacturer's or trade names does not constitute an official endorsement or approval of the use thereof.

Destroy this report when it is no longer needed. Do not return it to the originator.



Microelectromechanical System (MEMS) Gyroscope Noise Analysis and Scale Factor Characterization over Temperature Variation

by Angela Maio, Ryan Knight, and William Nothwang
Sensors and Electron Devices Directorate, ARL

REPORT DOCUMENTATION PAGE				Form Approved OMB No. 0704-0188	
<p>Public reporting burden for this collection of information is estimated to average 1 hour per response, including the time for reviewing instructions, searching existing data sources, gathering and maintaining the data needed, and completing and reviewing the collection information. Send comments regarding this burden estimate or any other aspect of this collection of information, including suggestions for reducing the burden, to Department of Defense, Washington Headquarters Services, Directorate for Information Operations and Reports (0704-0188), 1215 Jefferson Davis Highway, Suite 1204, Arlington, VA 22202-4302. Respondents should be aware that notwithstanding any other provision of law, no person shall be subject to any penalty for failing to comply with a collection of information if it does not display a currently valid OMB control number.</p> <p>PLEASE DO NOT RETURN YOUR FORM TO THE ABOVE ADDRESS.</p>					
1. REPORT DATE (DD-MM-YYYY) July 2016		2. REPORT TYPE Final		3. DATES COVERED (From - To) May–September 2015	
4. TITLE AND SUBTITLE Microelectromechanical System (MEMS) Gyroscope Noise Analysis and Scale Factor Characterization over Temperature Variation				5a. CONTRACT NUMBER	
				5b. GRANT NUMBER	
				5c. PROGRAM ELEMENT NUMBER	
6. AUTHOR(S) Angela Maio, Ryan Knight, and William Nothwang				5d. PROJECT NUMBER	
				5e. TASK NUMBER	
				5f. WORK UNIT NUMBER	
7. PERFORMING ORGANIZATION NAME(S) AND ADDRESS(ES) US Army Research Laboratory ATTN: RDRL-SER-L 2800 Powder Mill Road Adelphi, MD 20783-1138				8. PERFORMING ORGANIZATION REPORT NUMBER ARL-TR-7718	
9. SPONSORING/MONITORING AGENCY NAME(S) AND ADDRESS(ES)				10. SPONSOR/MONITOR'S ACRONYM(S)	
				11. SPONSOR/MONITOR'S REPORT NUMBER(S)	
12. DISTRIBUTION/AVAILABILITY STATEMENT Approved for public release; distribution is unlimited.					
13. SUPPLEMENTARY NOTES					
14. ABSTRACT Positioning, navigation, and timing estimation are critically important to Army systems from munitions to mounted and dismounted Soldiers. Gyroscopes provide information about angular orientation and are thus a necessary part of inertial measurement units for navigation systems. Because of noise and temperature changes, the sensor output can drift until the sensor data are no longer correlated to the system's orientation. If sensors provide inaccurate information, the location and orientation of the system are essentially unknown. To determine the reliability of gyroscopes' orientation information, we created methodologies to experimentally test and evaluate current and developing microelectromechanical system gyroscopes. The methodologies evaluate key metrics including angle random walk, bias instability, bias, and scale factor, and determine how each metric changes with environmental temperature. The results were verified by testing a commercial off-the-shelf gyroscope. These programs will be valuable for quantifying the magnitude of improvement in gyroscope stability and temperature sensitivity, and for performing thermal calibration.					
15. SUBJECT TERMS gyroscopes, microelectromechanical system, MEMS, inertial measurement units, Allan deviation, bias, scale factor, temperature variation					
16. SECURITY CLASSIFICATION OF:			17. LIMITATION OF ABSTRACT UU	18. NUMBER OF PAGES 36	19a. NAME OF RESPONSIBLE PERSON Angela Maio
a. REPORT Unclassified	b. ABSTRACT Unclassified	c. THIS PAGE Unclassified			19b. TELEPHONE NUMBER (Include area code) (301) 394-0728

Contents

List of Figures	iv
List of Tables	v
1. Introduction	1
1.1 Allan Deviation	2
1.2 Scale Factor and Bias	4
2. Experimental Approach	4
2.1 Allan Deviation Experiment	5
2.2 Scale Factor and Bias Experiment	8
3. Results	9
3.1 Allan Deviation	10
3.2 Scale Factor and Bias	14
3.3 ARW Comparison in Matlab	18
4. Conclusions	20
5. Future Work	21
6. References	23
Appendix. Angle Random Walk (ARW) Data	25
List of Symbols, Abbreviations, and Acronyms	27
Distribution List	28

List of Figures

Fig. 1	Sample plot representing Allan deviation separated by noise types, with bias instability (τ^0) and ARW ($\tau^{1/2}$) regions. (Reprinted from Time and Frequency from A to Z; Gaithersburg (MD): National Institute of Standards Technology's Physical Measurement Laboratory; 2010 May 12 [accessed 2016 Mar 25]. http://www.nist.gov/pml/div688/grp40/glossary.cfm .).....	3
Fig. 2	ACUTRONIC rate table and temperature chamber setup for gyroscope testing.....	5
Fig. 3	PinPoint gyroscopes mounted for Allan deviation testing.....	6
Fig. 4	Allan deviation program front panel in LabVIEW	7
Fig. 5	Scale factor program front panel in LabVIEW	9
Fig. 6	Allan deviation results for three PinPoint gyroscopes at 25 °C (averaged over 5 trials)	10
Fig. 7	Allan deviation graph from the PinPoint CRM100 datasheet (image courtesy of Silicon Sensing Systems Limited)	11
Fig. 8	Allan deviation graphs for one PinPoint gyro over its operating temperature range (averaged over 5 trials)	12
Fig. 9	Bias instability over temperature graphs for one PinPoint gyro (averaged over 5 trials, ± 1 STD error bars)	13
Fig. 10	ARW over temperature graph for one PinPoint gyro (averaged over 5 trials, ± 1 STD error bars)	13
Fig. 11	Bias over temperature plot for 3 PinPoint gyroscopes tested (averaged over 5 trials, ± 1 STD error bars)	15
Fig. 12	Bias over temperature from the PinPoint CRM100 datasheet (image courtesy of Silicon Sensing Systems Limited)	16
Fig. 13	Scale factor over temperature for 3 PinPoint gyroscopes tested (averaged over 5 trials, ± 1 STD error bars)	17
Fig. 14	Scale factor error over temperature from the PinPoint CRM100 datasheet (image courtesy of Silicon Sensing Systems Limited).....	18
Fig. 15	ARW calculated from trial 1 Allan deviation data, using LabVIEW (1-s approximation) and Matlab (best fit).....	19
Fig. 16	ARW calculated from trial 2 Allan deviation data, using LabVIEW (1-s approximation) and Matlab (best fit).....	19

List of Tables

Table 1	Gyroscope parameters as published by manufacturers of COTS and state-of-the-art gyroscopes.....	2
Table 2	Evaluation parameters collected by our LabVIEW programs compared to manufacturer data for the PinPoint	10
Table 3	Rate random walk ($^{\circ}/h^{3/2}$) calculated using Matlab	20
Table A-1	ARW over temperature as calculated by LabVIEW (1-s approximation) and Matlab (best fit), Trial 1	26
Table A-2	ARW over temperature as calculated by LabVIEW (1-s approximation) and Matlab (best fit), Trial 2	26

INTENTIONALLY LEFT BLANK.

1. Introduction

Microelectromechanical system (MEMS) gyroscopes provide information about angular orientation without requiring an external signal by observing an angular change. As a result, they are valuable for positioning, navigation, and timing (PNT) applications for the Army. Three axes of navigation-grade gyroscopes in combination with 3 axes of accelerometers form an inertial measurement unit (IMU), which can aid or replace GPS for PNT applications. When the gyroscopes' measured angular velocities are integrated and the accelerometers' measured accelerations are double integrated, the IMU is capable of providing GPS-like position information. Use of IMUs with MEMS gyroscopes decreases the vulnerability of PNT systems by eliminating the threats of signal loss and jamming.

MEMS gyroscopes have been successfully characterized using Allan deviation and scale factor methods. The error parameters found using these methods, such as bias instability, angle random walk (ARW), and scale factor linearity error, are useful for determining the reliability of the gyroscope as an angular orientation sensor. They provide information about how much the gyroscope signal drifts with zero input angular rate, as well as the scale factor's predictability with different input rates. There are also methods to determine gyroscope stability with changes in surrounding temperature, which is the focus of this project.^{1,2}

Some commercial off-the-shelf (COTS) gyroscopes have Allan deviation and scale factor parameters available, even at different temperatures and with temperature calibration data. However, the manufacturers' test methods are unreported and parameters are not always up to date.³ In addition, many state-of-the-art gyroscopes are minimally tested, and temperature data are often unavailable (Table 1). As a result, there is a need for a standard set of test methods and programs, especially to perform initial characterizations of gyroscopes built in-house. This project succeeded in creating test protocol and LabVIEW programs to characterize gyroscopes' performance with temperature and consistently produce results that match the manufacturers' reported parameters.

Table 1 Gyroscope parameters as published by manufacturers of COTS and state-of-the-art gyroscopes⁴⁻⁷

Gyroscope/IMU	Bias instability (°/h)	ARW (°/√h)	Bias sensitivity ([°/h]/°C)	Scale factor sensitivity (%/°C)
PinPoint	24	0.28	±43.2 ^a	±0.008 ^b
SIMS SRG	0.05	0.3 ^c	1	0.002 ^d
LandMark 40 IMU	6	0.12 ^e	0.576 ^f	≤0.0008 ^g
STIM210	0.5	0.15	9	NA

^aCalculated from manufacturer-reported “bias over temperature” of ±1.5°/s (assumed to be over full temperature range).

^bCalculated from manufacturer-reported “SF over temperature” of ±1% (assumed to be over full temperature range).

^cUnits converted from manufacturer-reported ARW of 0.005°/h/√Hz.

^dListed by manufacturer as “temperature coefficient” percent of full scale per °C.

^eUnits converted from manufacturer-reported ARW of 0.002°/s/√Hz.

^fCalculated from manufacturer-reported bias (over temp.) difference of 0.02°/s (assumed to be over full temperature range).

^gCalculated from manufacturer-reported “scale factor error (over temperature) 1σ” of ≤0.1% (assumed to be over full temperature range).

^hCalculated from manufacturer-reported “bias error over temperature” of 9°/h (rms on residuals over the temperature range).

Note: SIMS SRG = Sensors in Motion Symmetrical Resonating Gyroscope.

1.1 Allan Deviation

When a gyroscope has no angular rate applied, the average output is called the bias. Over time, the bias can drift despite the gyroscope not moving. Thermal fluctuations, die attachment, and printed circuit board (PCB) stresses can all contribute to bias drift. Allan deviation is a measure of how much a gyroscope signal drifts over time. The Allan variance for the corresponding τ (bin size) is represented by Eq. 1.

$$\sigma^2(\tau) = \frac{1}{2} \langle (\bar{\omega}_{i+1} - \bar{\omega}_i)^2 \rangle. \quad (1)$$

In the equation, $\sigma^2(\tau)$ is the Allan variance, τ represents bin width, and $\bar{\omega}$ is the average rotation rate from each bin.¹ The square root of the Allan variance, called the Allan deviation in degrees per hour, is plotted logarithmically with respect to τ . A sample plot of Allan deviation is shown in Fig. 1.

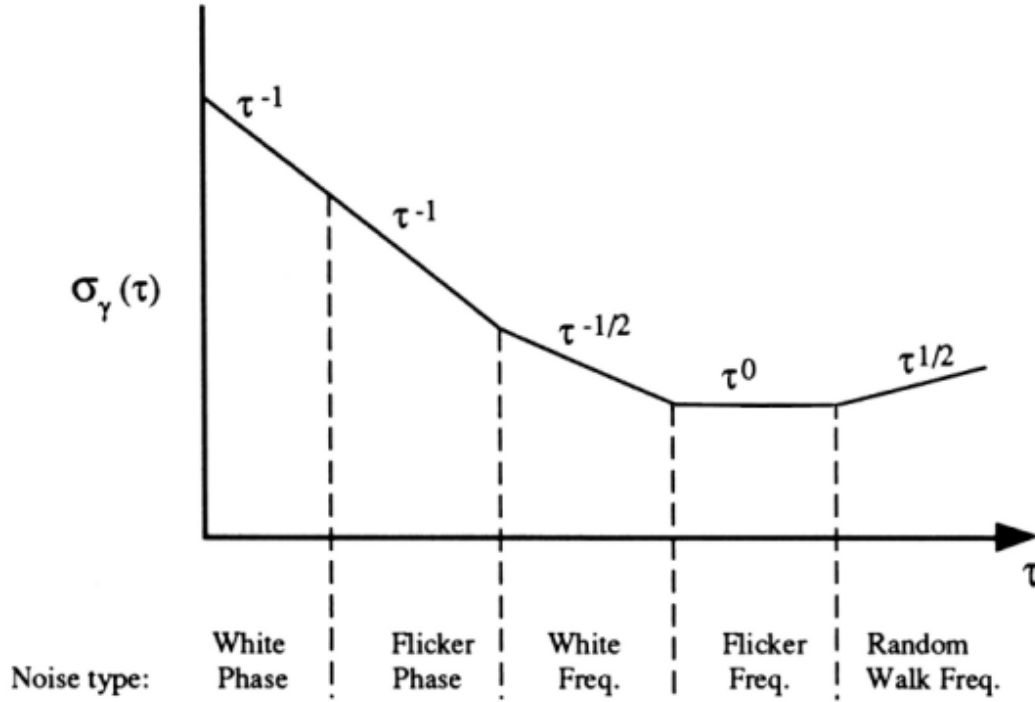


Fig. 1 Sample plot representing Allan deviation separated by noise types, with bias instability (τ^0) and ARW ($\tau^{-1/2}$) regions. (Reprinted from *Time and Frequency from A to Z*; Gaithersburg (MD): National Institute of Standards Technology's Physical Measurement Laboratory; 2010 May 12 [accessed 2016 Mar 25]. <http://www.nist.gov/pml/div688/grp40/glossary.cfm>.)

The *bias instability* is the minimum value of Allan deviation on the logarithmic plot, expressed in degrees per hour. It represents how much the gyroscope's bias will drift in a given time window due to flicker noise. For example, a gyroscope with $1^\circ/\text{h}$ bias instability occurring at a 1,000-s τ value will have a signal that may drift by $1^\circ/\text{h}$ in any data set of 1,000 s.⁸ In the sample Allan deviation plot (Fig. 1), the bias instability is within the range indicated by τ^0 , where the slope of the Allan deviation is 0.

ARW is a measure of white noise introducing error into the gyroscope's rate signal and can be found using the best fit line of the Allan deviation plot with a slope of $-1/2$, as shown in Fig. 1. The ARW associated with any bin size is represented in Eq. 2, in which τ is the bin size, σ is the corresponding Allan variance (Eq. 1), and N is the ARW in degrees per root hour:

$$N = \sqrt{\tau} * \sigma(\tau). \quad (2)$$

For this project, we are interested in how error parameters, namely bias instability and ARW, change with temperature. This will tell us the reliability of a gyroscope's signal at various environmental temperature conditions.

1.2 Scale Factor and Bias

The gyroscope signal must be multiplied by a scale factor to convert from voltage to angular rate using Eq. 3, where ω is the measured angular rate, k is the scale factor, and V_{out} is the zeroed voltage output from the gyroscope:

$$\omega = k * V_{out}. \quad (3)$$

For the gyroscope output to be zeroed, we must subtract the bias (average zero-rate output) from the signal. Both the bias and the scale factor have associated error.

The scale factor's variation with angular rate is called the scale factor linearity error in parts per million.² Information about how the linearity error was calculated in the LabVIEW programs is available in the US Army Research Laboratory report *Characterization of MEMS Gyroscopes for Navigation Grade Inertial Measurement Units*.³ The scale factor also varies with temperature. If the gyroscope's nominal scale factor is used to calculate the angular rate measurement at a temperature that differs from the nominal, then the scale factor variation will introduce error into the measurement. Fortunately, the variation can be measured and used to calibrate the gyroscope for different temperatures. One of the goals of the scale factor test will be to determine both the nominal scale factor and the scale factor at other temperatures within each gyroscope's operating range.

The bias sensitivity (in volts per degrees Celsius) is found by plotting the average bias at each temperature, computing a least mean squares fit, and finding the slope of the best fit line. The slope can then be used as the bias sensitivity constant to calibrate for any known temperature within the gyroscope's performance range. The bias sensitivity coefficient can be multiplied by the measured temperature of the gyroscope and subtracted from the signal in order to calibrate the sensor.

2. Experimental Approach

The lack of consistent procedures to characterize MEMS gyroscope performance with temperature changes prompted us to create these programs to test and evaluate gyroscopes. We tested the programs using the following methods to determine their reliability.

A rate table and temperature chamber setup created by ACUTRONIC (Fig. 2) was used for both experiments. The developed LabVIEW programs controlled both the rate table and the temperature chamber via serial communication, setting the appropriate spin rate and temperature at different points of the tests.



Fig. 2 ACUTRONIC rate table and temperature chamber setup for gyroscope testing

To set up each test, the user selects the channels to read from the data acquisition (DAQ) unit and provides the input, nominal, and output voltages as well as the nominal scale factor from the gyroscope datasheets. The user also sets the sample rate, temperatures, and test times, including warmup time for the analog-to-digital converter and temperature settling time, before starting the experiment. While the program is running, it displays the current status of the test, the set temperature, and time elapsed at each step of the test, as well as graphs and data that vary between programs (to be discussed separately in the following sections).

2.1 Allan Deviation Experiment

For the Allan deviation test, each gyroscope was mounted on the rate table (Fig. 3). The 3-axis CRM100/200 evaluation board on the left was used for preliminary validation of the test setup. The 3 single-axis CRM100 evaluation boards were used for further testing and characterization of the PinPoint. The rate table axis was enabled to keep the gyroscope in a stable position with no input angular rate for the duration of the experiment. The temperature chamber was sealed and set to vary the temperature according to the program's instructions, so that Allan deviation parameters could be collected at various temperatures within each gyroscope's

performance range. The programs calculated bias instability and ARW at each temperature, then plotted them so the gyroscope's performance within the temperature range could be easily viewed and compared.

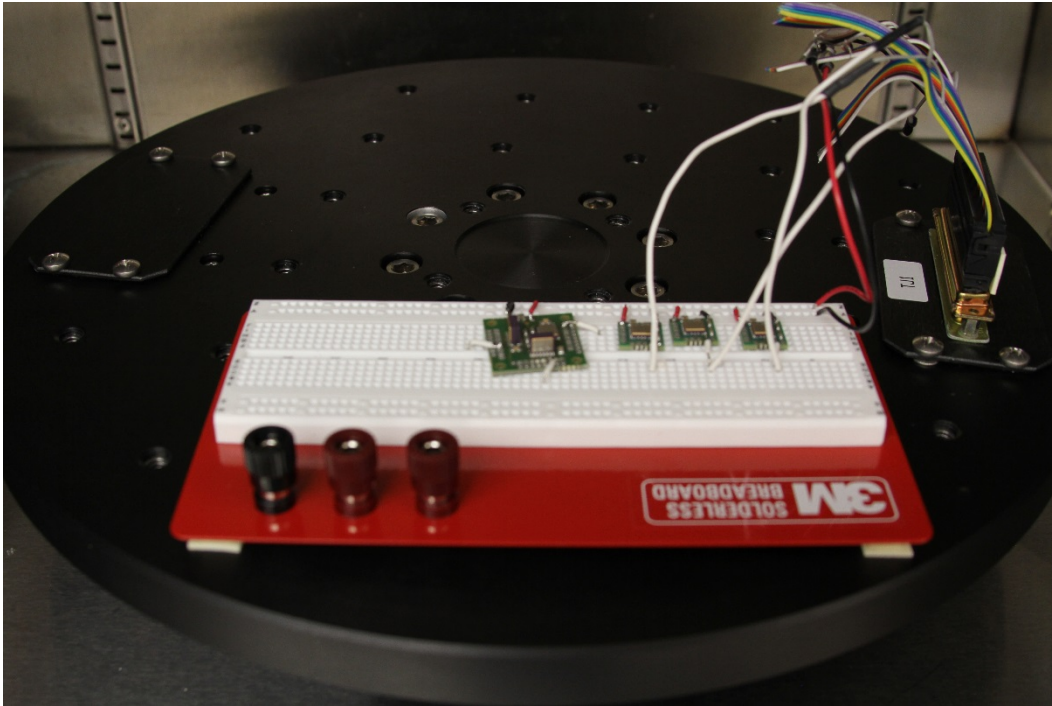


Fig. 3 PinPoint gyroscopes mounted for Allan deviation testing

Each gyroscope was powered with a DC power supply at the voltage suggested by its manufacturer's specification sheet. The output was measured using a BNC-2110 National Instruments DAQ system.

The LabVIEW virtual instrument plotted quasi-real-time Allan deviation curves by reading from the DAQ. It could collect data from up to 8 channels at once to allow for simultaneous testing of multiple gyroscopes. Data was sampled at 10,000 Hz (set with a user-changeable sampling rate) and averaged to determine the Allan deviation for each bin size. For bin sizes larger than 1 s, the averages were calculated recursively to reduce computational load. A subVI within the program split the data from each channel into bins of size τ and recursively averaged the data within each bin by checking whether the size of the data collected was greater than the bin size. If the data size was greater, the program split the data into tau-sized arrays, averaged each array, and stored each average in the mean buffer. If the data were not enough to fill the bin, the recursive average was calculated until the bin was filled and the mean could be stored in the mean buffer. Another subVI took the difference between successive averages, squared the differences, and found half of the average of these values. The square root of the final value was stored in the

Allan deviation buffer. The subVI also stored the total number of averages calculated for each bin size. If there were 10,000 or more averages, the subVI locked the Allan deviation value and stopped calculating averages to reduce the memory load on the system.

The Allan deviation method, bias instability, and ARW calculations in this program are detailed further in previous work.³ The only major change to the method was the ARW calculation. In the previous program, the ARW was calculated through line fitting, which provided inconsistent values. The new program obtains the ARW by finding the Allan deviation at the point where tau is equal to 1 s. This estimate is much more consistent. The program saves the Allan deviation data for each temperature, so the user has the option to calculate the ARW using another method in MATLAB or a program of their choosing.

The program front panel is pictured in Fig. 4, with a section to set up the test as well as displays of the bias instability and ARW over temperature graphs, and current Allan deviation graphs for each channel.

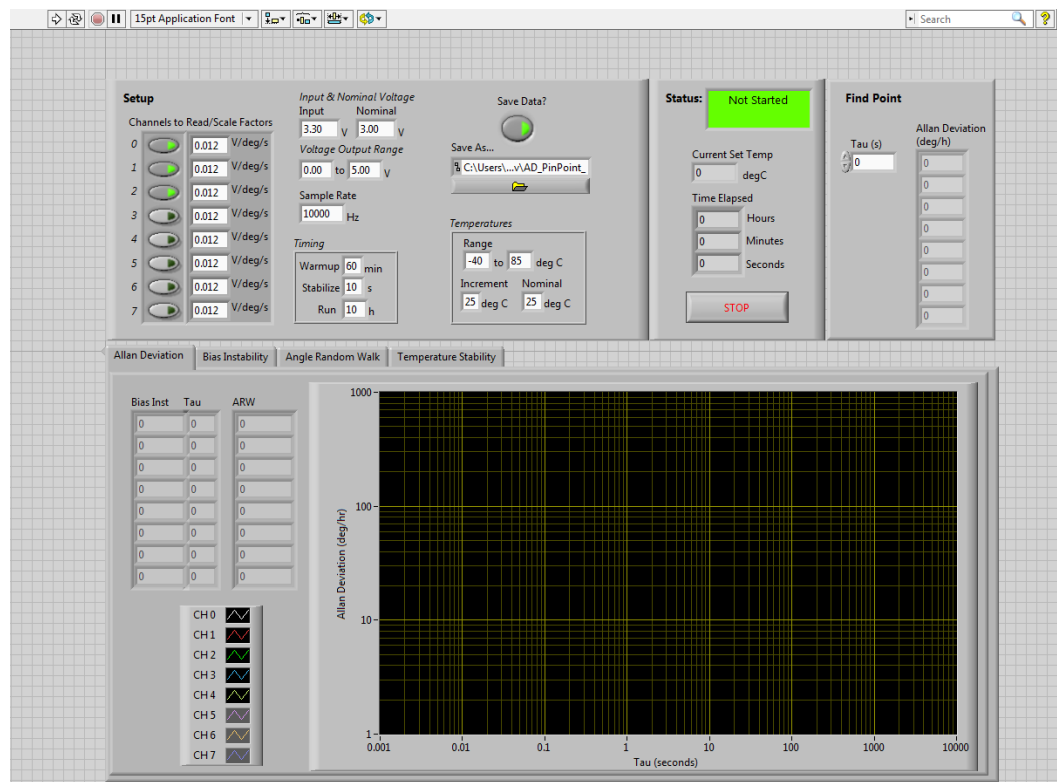


Fig. 4 Allan deviation program front panel in LabVIEW

2.2 Scale Factor and Bias Experiment

For the scale factor and bias test, each gyroscope was mounted on the rate table inside the temperature chamber and spun at different user-defined rates while the temperature was constant. The program ran the same rate test at various set temperatures to determine how the surrounding temperature would affect the gyroscope's scale factor and bias. This helped us to determine a bias sensitivity constant, which can be used to calibrate the gyroscope based on its surrounding temperature, assuming the relationship between bias and temperature is approximately linear.

The LabVIEW program used the same scale factor and linearity error determination process as the previous code but added temperature change as a factor to determine the scale factor and bias sensitivities to temperature. The rate table was set to run at several rates throughout each gyroscopes' range, for 100 s each. The 100-s averaging time was chosen because it was the approximate value of the tau bin size at the bias instability point in previous Allan deviation tests. This point is representative of the averaging time that will include the least bias instability error. After each 100-s run at a rate, the rate table would accelerate to the next rate and begin another 100-s average of the gyroscope output. The scale factor was calculated as the slope of the least mean squares fit of the output versus angular rate plot. The program ran through the user-specified rate range twice (once from the lowest rate to the highest rate, then back down), then averaged the 2 calculated scale factor values.

Once the program finished calculating the scale factor, the temperature chamber's set point was changed, the chamber was allowed to heat or cool to the desired temperature, and the rate test was started again. The program front panel is shown in Fig. 5.

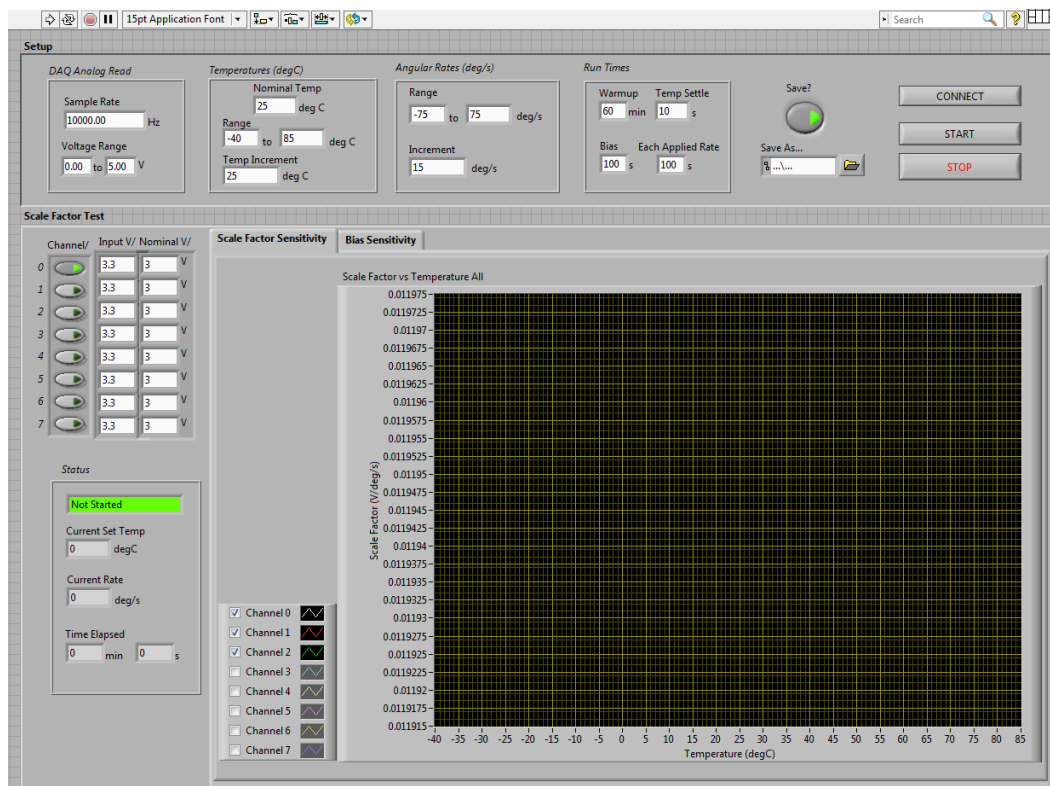


Fig. 5 Scale factor program front panel in LabVIEW

For each temperature, the measured scale factor was plotted and displayed to the user in the scale factor over temperature graph.

The program also recorded the gyroscope bias in volts and plotted the value for each temperature. It calculated the linearity error for the bias sensitivity graph by determining the deviation of the bias from the best fit line. The slope of the best fit line was calculated as the bias sensitivity, in volts per degrees Celsius. Knowledge of the linearity of the graph provided a measure for how accurate the bias sensitivity would be as a calibration constant. If the plot was mostly linear, we could conclude that the sensitivity could be used for bias calibration.

3. Results

From the Allan deviation and scale factor data collected and processed by our LabVIEW programs for each gyroscope, we found that the gyroscopes were characterized by the values shown in Table 2 at the nominal temperature of 25 °C.

Table 2 Evaluation parameters collected by our LabVIEW programs compared to manufacturer data for the PinPoint

	Bias instability (°/h)	ARW (°/√h)	Bias (V)	Scale factor (V/°/s)
Expected⁴	7.2 ^a	0.18	1.65 ^b	0.012
Measured	6.401	0.1848	1.653732	0.011952

^aAllan deviation value taken at tau = 10 s.

^bCalculated based on manufacturer reported bias = $V_{dd}/2$, where supply voltage is 3.3 V.

3.1 Allan Deviation

Allan deviation plots for 3 PinPoint gyroscopes tested over 10 h indicate a bias instability of about 6.4°/h and an ARW of 0.18°/√h at the nominal temperature (Fig. 6). The following plot has each gyroscope's Allan deviation data for 5 trials averaged together.

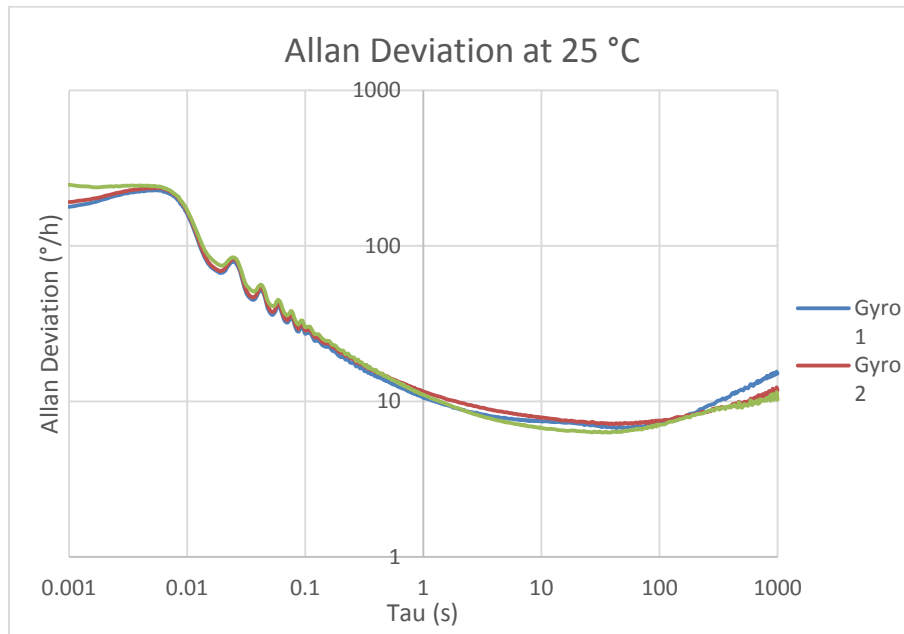


Fig. 6 Allan deviation results for three PinPoint gyroscopes at 25 °C (averaged over 5 trials)

The plots are similar to the one provided in the gyroscope's datasheet. The peaks in our plots between tau 0.01 and 0.1 s indicate the frequency of the 60-Hz power supply. The signal appears clearly and predictably, and is ignorable because we are primarily interested in the later portions of the Allan deviation curve, where the ARW and bias instability are determined.

The following graph (Fig. 7) from the PinPoint CRM100 datasheet is comparable to our plots, noting that the Allan deviation is now given in degrees per second, as opposed to degrees per hour. The ARW is stated as $0.18^\circ/\sqrt{h}$, very similar to our results. Silicon Sensing indicates that the curve is down to $0.002^\circ/s$ ($7.2^\circ/h$) at an approximate tau value of 10 s, which is $0.8^\circ/h$ from our recorded bias instability. This is likely due to Silicon Sensing's approximation of 10 s as the bias instability point. Our Allan deviation has similar values around 10 s, but the curve continues to decrease to arrive at the bias instability around 60 s.

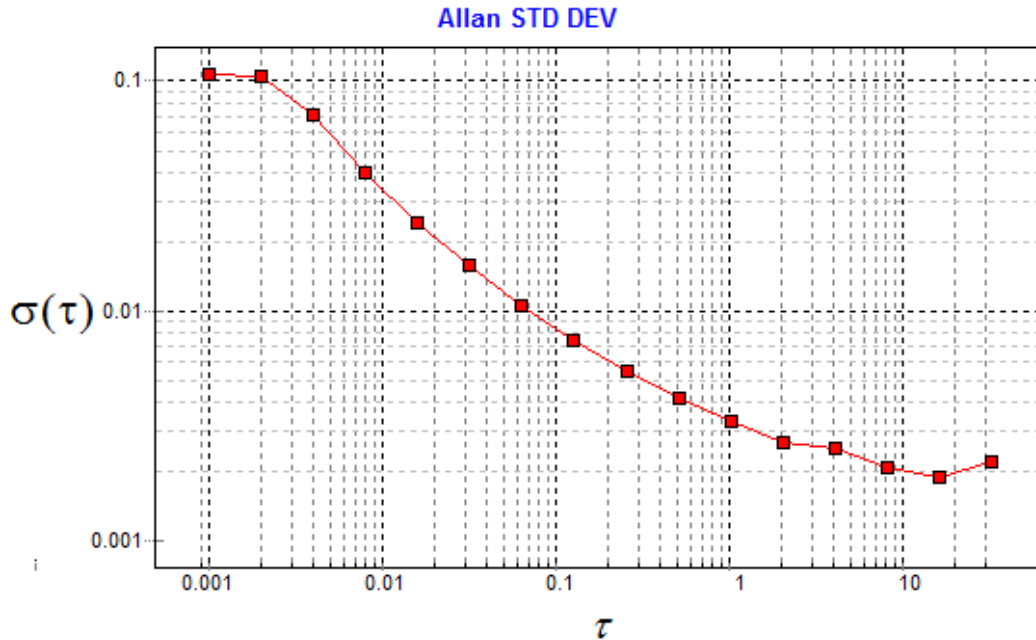


Fig. 7 Allan deviation graph from the PinPoint CRM100 datasheet⁴ (image courtesy of Silicon Sensing Systems Limited)

After verifying the LabVIEW results for Allan deviation at the nominal temperature of 25 °C, we move on to consider the results at different temperatures within the PinPoint gyroscope's operating range. The following graph (Fig. 8) shows the Allan deviation results of one gyroscope over 7 temperatures in the operating range of -40 to 85 °C. We chose to display the results of only one gyroscope for simplicity. These results are representative of the results for the 3 gyroscopes tested.

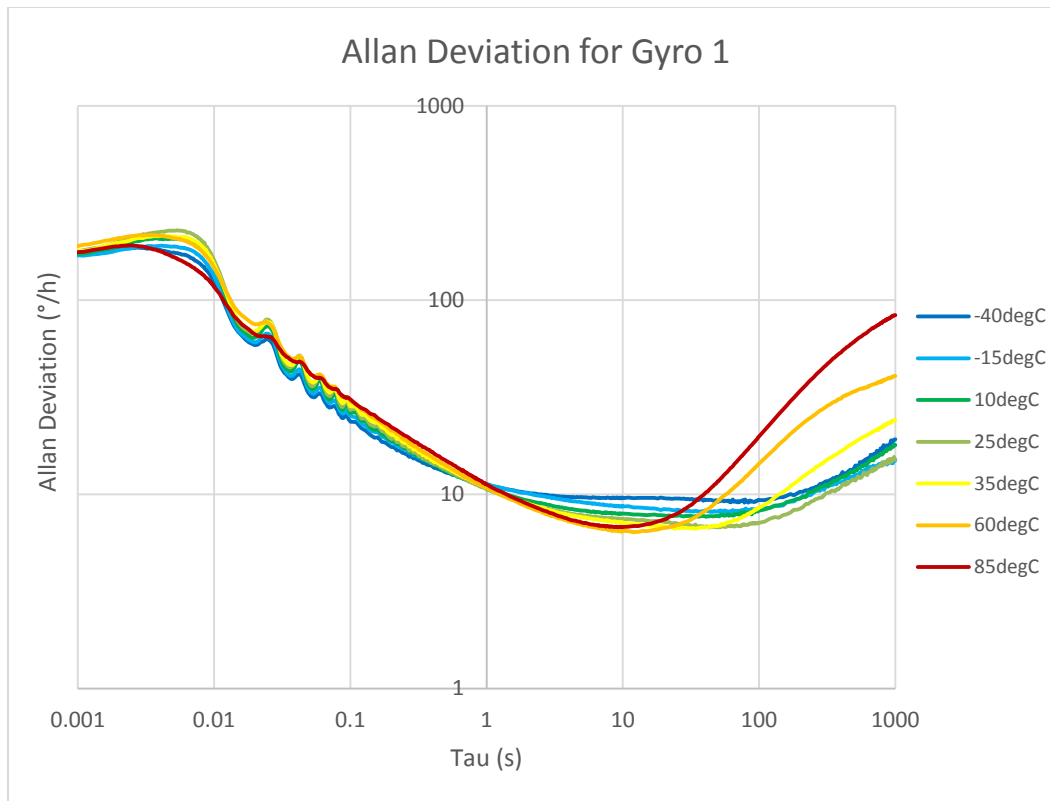


Fig. 8 Allan deviation graphs for one PinPoint gyro over its operating temperature range (averaged over 5 trials)

The Allan deviation shows a tendency to increase at higher averaging times when the gyroscope is subjected to higher temperatures. In addition, the Allan deviation between tau values of 0.01 and 0.1 s fluctuates more at lower temperatures (likely due to 60-Hz fluctuations). These fluctuations indicate low-frequency noise caused by improper grounding inside the rate table's slip rings. This noise does not affect the calculations of bias instability and ARW, which are taken from points farther to the right in the Allan deviation curve. The bias instability point seems to move to lower averaging times (shifting to the left) as the temperature increases. We can assume gyroscope performance, as measured by bias instability, will be reduced at temperatures below 25 °C by examining the graph. The ARW, on the other hand, appears to be fairly constant, as all curves converge at a tau value of 1 s. We may analyze the bias instability and ARW over temperature further by plotting them directly as in Figs. 9 and 10.

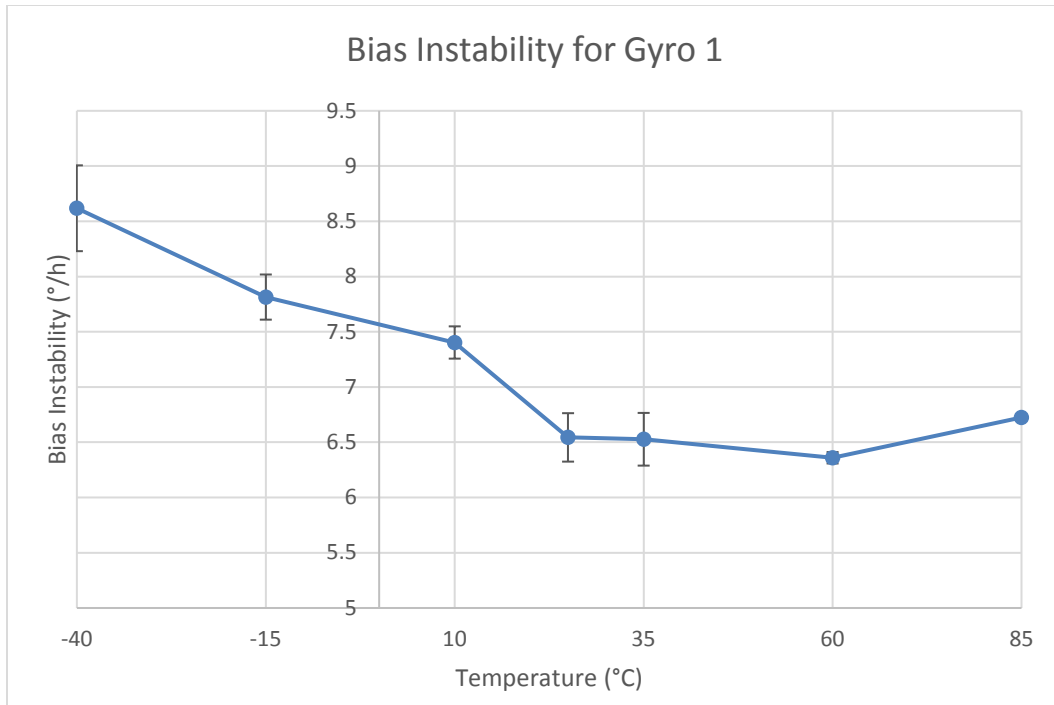


Fig. 9 Bias instability over temperature graphs for one PinPoint gyro (averaged over 5 trials, ± 1 STD error bars)

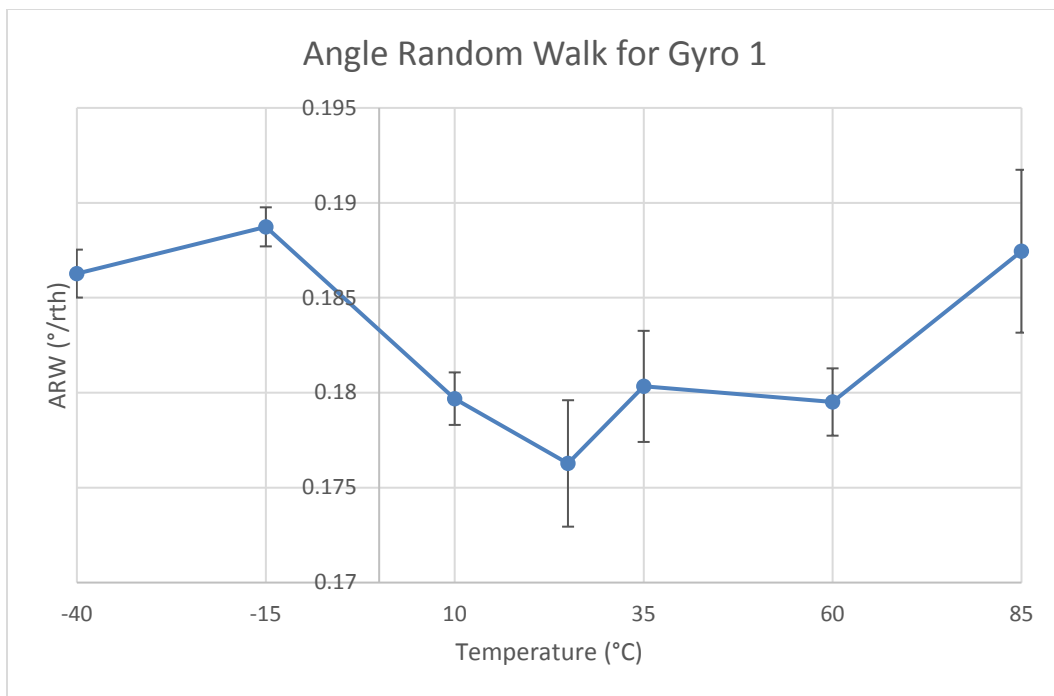


Fig. 10 ARW over temperature graph for one PinPoint gyro (averaged over 5 trials, ± 1 STD error bars)

The error bars indicate $\pm 1\sigma$ over the 5 trials. Figure 9 indicates that the lowest bias instability for the gyroscope is $6.36^\circ/\text{h}$, occurring at a temperature of 60°C . There is also less variability in the bias instability measurements at higher temperatures of 60 and 85°C . The bias instability is highest at temperatures below the nominal, indicating that the gyroscope bias will drift more at lower temperatures. In fact, the bias instability at -40°C is $1.4^\circ/\text{h}$ higher than the manufacturer's reported bias instability. This indicates that the gyroscope may not be performing according to its specifications at all points in the recommended temperature range.

The ARW plotted in Fig. 10 is shown to be lowest at the gyroscope's nominal temperature of 25°C . At this point, the ARW is approximately $0.176^\circ/\sqrt{\text{h}}$. At its highest value, the ARW is $0.0087^\circ/\sqrt{\text{h}}$ (about 5%) higher than the manufacturer's reported value. However, the large amount of standard deviation between trials (indicated by the error bars) when the temperature is over 25°C indicates that the change in ARW over temperature is not statistically significant at higher temperatures.

In the future, the LabVIEW test setup could be used to test over smaller temperature ranges that provide the lowest bias instability and ARW values. This points to the usefulness of the Allan deviation program as a tool to determine the ideal temperature conditions for each gyroscope.

3.2 Scale Factor and Bias

The scale factor experiment produced results for bias sensitivity and scale factor sensitivity, as well as a linearity error graph for bias. The linearity error plot ideally shows the amount of error obtained by approximating the sensitivity value as the slope of the best fit line. Lower linearity error values for bias sensitivity indicate that by multiplying the sensitivity coefficient by the current measured temperature, then subtracting that voltage value from the analog voltage gyroscope signal, we will obtain a more accurate angular rate measurement. The PinPoint gyroscope we tested already has bias compensation through its temperature sensor, so the bias-temperature relationship is highly nonlinear, as shown in Fig. 11. The data for each gyroscope were averaged between 5 trials.

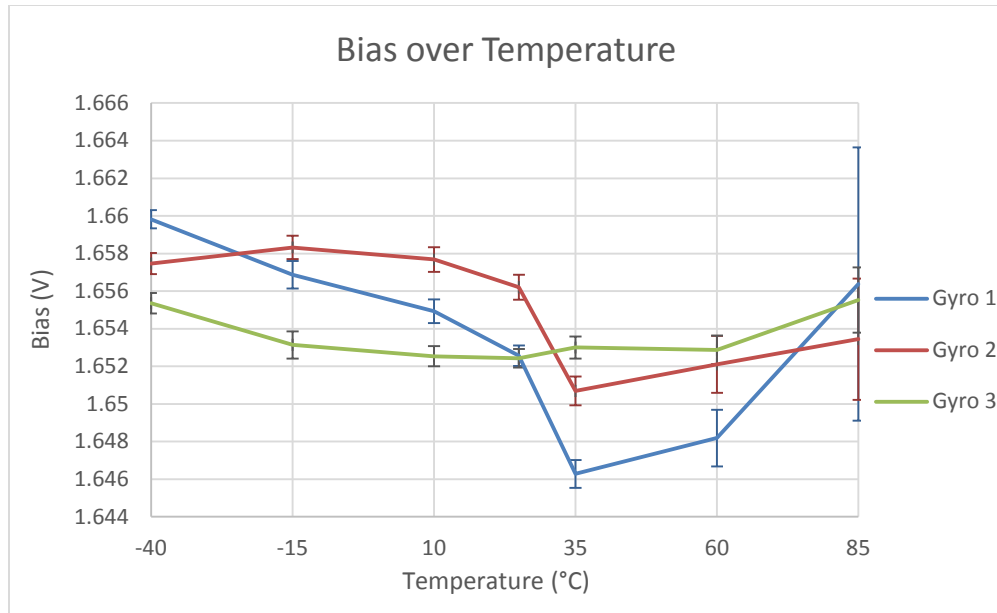


Fig. 11 Bias over temperature plot for 3 PinPoint gyroscopes tested (averaged over 5 trials, ± 1 STD error bars)

This plot shows a nonlinear trend due to the bias compensation integrated in the PinPoint. The bias varies more between trials in the higher temperature range, as indicated by the larger error bars. In addition, the bias has almost twice as much variation between individual gyroscopes as between trials. Variations between trials are about ± 2 mV (1σ), whereas the variation of bias in different gyroscopes is up to 7 mV at the same temperature. This indicates that our results are relatively precise, despite possible measurement errors. Sources of measurement error contributing to the ± 2 mV bias fluctuation include fluctuations in the power source, noise added by the rate table's slip ring, applied rate inaccuracy, and data acquisition error.

We can compare our results to the graphs provided in the datasheet. The bias seems to be calculated at only 3 temperatures: -40 , 25 , and 85 °C. The gyroscopes were tested with an input voltage of 3 V instead of our 3.3 V, which explains the shift between the 2 bias graphs. The bias is indicated to be half of the input voltage, so our values are still in agreement with the specifications. The manufacturer's bias graph does not provide much to compare due to the lack of incremental temperature tests, but it does indicate that there is less variation of bias at the nominal temperature (Fig. 12). Also, the approximate variation of bias from the nominal is between 0 and ± 30 mV. Our results agree with the manufacturer based on a maximum variation of approximately 14 mV when 3 gyroscopes were tested. If more gyroscopes were tested, we would likely find a larger overall variation similar to the plot shown in Fig. 12.

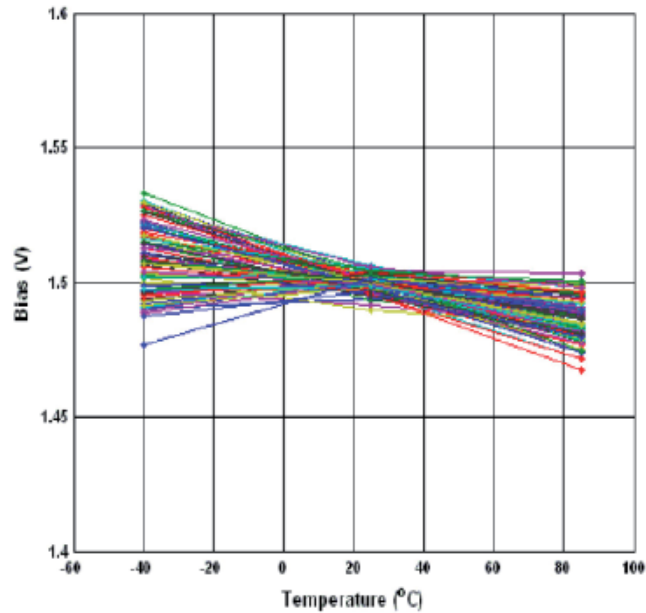


Fig. 12 Bias over temperature from the PinPoint CRM100 datasheet⁴ (image courtesy of Silicon Sensing Systems Limited)

More importantly, the manufacturer's ± 30 mV variations are much larger than our ± 2 mV variation between trials, indicating that the test method's error is well within the error reported by the manufacturer. As a result, these tests could be used to create a more refined model to further reduce gyroscope bias variation. The model is discussed in Section 4.

We can also see the amount of variation in the scale factor by looking at the following plot over temperature, averaged between 5 trials (Fig. 13). This shows a trend toward lower scale factors at higher temperatures. (The actual scale factors measured are slightly below the manufacturer's nominal value of 0.012 V/°/s.)

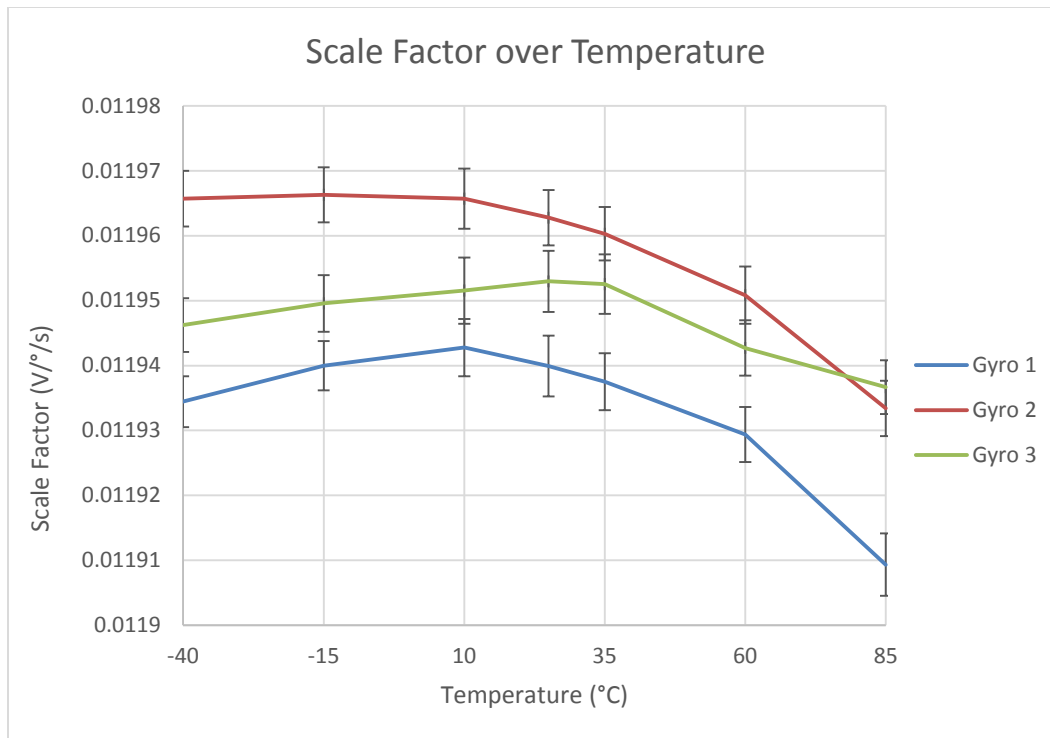


Fig. 13 Scale factor over temperature for 3 PinPoint gyroscopes tested (averaged over 5 trials, ± 1 STD error bars)

The scale factor plot provided by the manufacturer is a graph of scale factor error, in percent (Fig. 14), instead of the general scale factor. We can still use this for comparison by noticing that there is a tendency toward positive error at low temperatures and negative error at high temperatures. Our results indicate a constant negative error when compared to the nominal scale factor provided and also a larger negative error at higher temperatures. However, our plot does not appear to have positive error at low temperatures when considering the 3 gyroscopes tested.

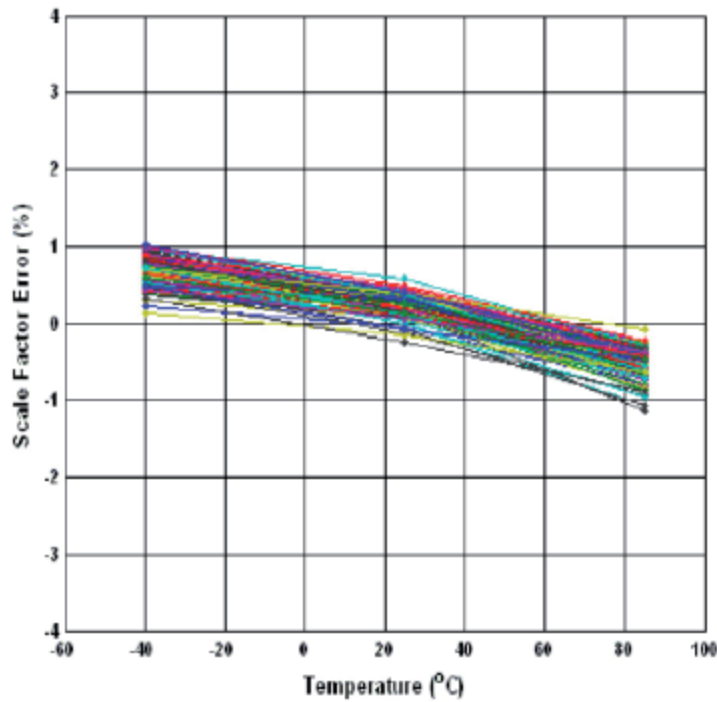


Fig. 14 Scale factor error over temperature from the PinPoint CRM100 datasheet⁴ (image courtesy of Silicon Sensing Systems Limited)

The scale factor error of our results is confined within the manufacturer's specified error. The manufacturer shows a maximum $\pm 1\%$ scale factor variation, whereas our plots indicate a variation from the nominal of approximately -0.3% to -0.75% . In addition, the 1σ variation between trials is less than 0.1% as indicated by the error bars. This indicates that our test results could be used to create a better model to calibrate individual gyroscopes' scale factor based on the measured temperature.

3.3 ARW Comparison in Matlab

To determine the validity of our LabVIEW program's ARW approximation (Allan deviation value when tau is equal to 1 s), we analyzed 2 trials of Allan deviation data in Matlab and calculated the ARW in a different manner. The Matlab program used the 1-s tau bin as an initial estimate for the ARW, created a line with a slope of $-1/2$, and then checked the intersection points of the line with the Allan deviation graph. It adjusted the position of the $-1/2$ line, optimizing the line to best fit the Allan deviation curve. The ARW estimates using the LabVIEW and Matlab programs are displayed in Figs. 15 and 16. Tables of the values are also provided in the Appendix.

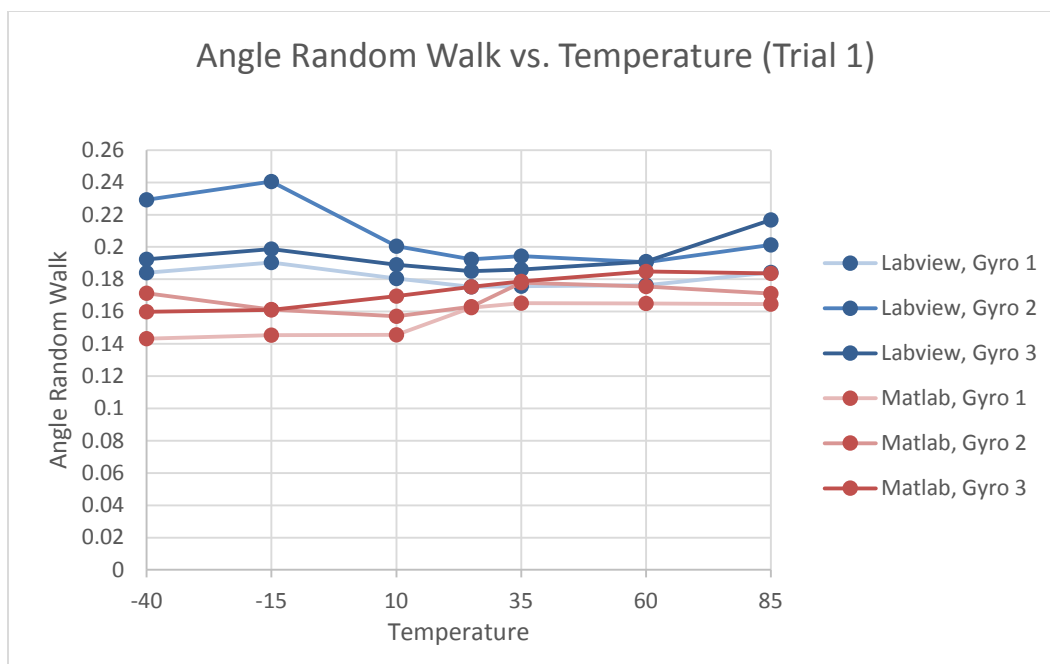


Fig. 15 ARW calculated from trial 1 Allan deviation data, using LabVIEW (1-s approximation) and Matlab (best fit)

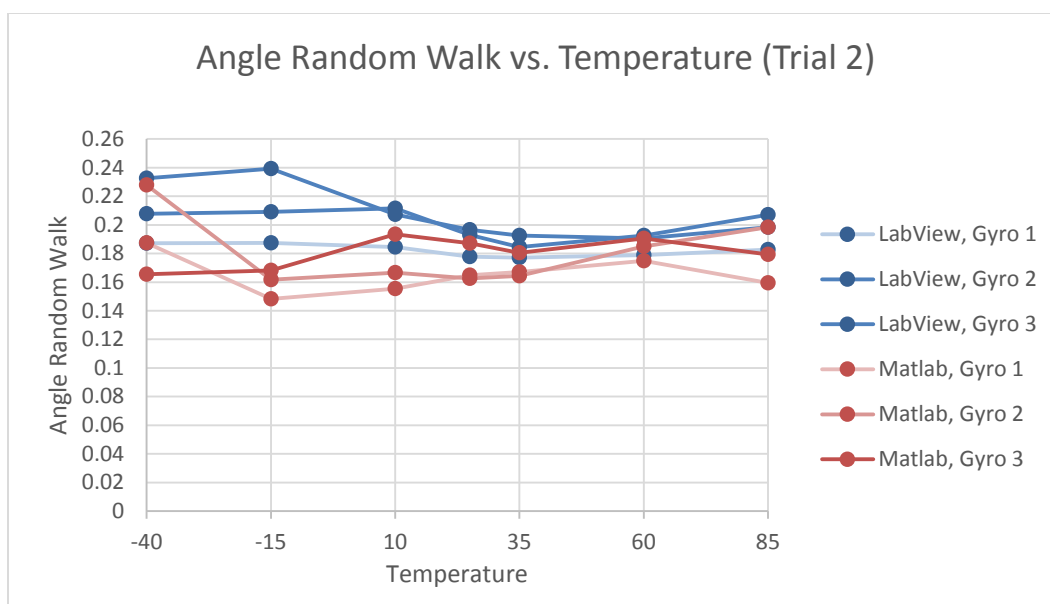


Fig. 16 ARW calculated from trial 2 Allan deviation data, using LabVIEW (1-s approximation) and Matlab (best fit)

In both trials, the Matlab calculation of ARW was consistently lower than the LabVIEW approximated value. This means that the Allan deviation graph reached a slope of $-1/2$ when the tau value was greater than 1 s. As a result, the $-1/2$ slope best fit calculated a lower ARW value than the 1-s tau approximation. The values were closest to each other just above the nominal temperature. Although the values are fairly close to each other for all temperatures (with an average difference of about $0.0248^\circ/\sqrt{h}$), the results from the 2 methods do not indicate the same trend over temperature. We can conclude that the variation of ARW over temperature is smaller than what can be measured using our 1-s tau approximation. The variation due to the approximation is greater than the variation due to temperature. Based on the comparison between the LabVIEW and Matlab calculations, the LabVIEW approximation is valid for determining an ARW value close to the actual value but is not accurate enough to determine a trend with temperature.

We also used Matlab to calculate the rate random walk for the same data using the same method as the ARW calculation. In this best fit optimization, the line was specified to have a slope of positive $1/2$ and the initial estimate was chosen as the Allan deviation value when tau was 3600 s, or 1 h. The results for both trials are presented in Table 3.

Table 3 Rate random walk ($^\circ/\text{h}^{3/2}$) calculated using Matlab

Temp	RRW, Gyro 1		RRW, Gyro 2		RRW, Gyro 3	
	Trial 1	Trial 2	Trial 1	Trial 2	Trial 1	Trial 2
-40	0.014953	0.012311	0.0079719	0.0076631	0.02155	0.0079268
-15	0.014824	0.014055	0.016892	0.015476	0.013824	0.011827
10	0.012874	0.013343	0.013558	0.012992	0.012593	0.011022
25	0.011261	0.010573	0.012269	0.012435	0.010328	0.01208
35	0.013531	0.014351	0.014417	0.012734	0.012853	0.01255
60	0.027711	0.019	0.026683	0.022697	0.013058	0.013042
85	0.040339	0.026022	0.042466	0.027297	0.014403	0.011953

We notice much more variation in the calculations of rate random walk. This is a result of the Allan deviation data being more varied between trials at larger tau bin sizes, because there are not as many bins to average when each bin requires minutes or hours of data.

4. Conclusions

Our nominal temperature results for bias instability, ARW, bias, and scale factor matched the manufacturers' specifications for each gyroscope consistently, with small differences due to testing variations between our procedure and the manufacturers'. We may conclude that the LabVIEW programs are reliable for

finding gyroscope error parameters for other temperatures based on their accuracy at the nominal temperature. However, a more complex ARW calculation may improve the accuracy in cases when the ARW cannot be approximated at a tau value of 1 s. This may be especially evident in tests of gyroscopes with much lower ARW values. We propose testing state-of-the-art gyroscopes to determine whether there are other issues with the test setup that may make it inaccurate for gyroscopes with less error. Possible issues include small (less than 1°) temperature fluctuations within the chamber and noise provided by the DC voltage supply. In addition, the rate table's input rate stability and accuracy may have an impact when testing navigation-grade gyroscopes. The current rate table's accuracy of 0.5 ppm (0.25 ppm clockwise or 0.53 ppm counterclockwise)⁹ allows the test setup to measure scale factor stabilities as low as 0.5 ppm. Gyroscopes with lower-scale factor stability values may be affected by input rate inaccuracies, leading to unreliable results for the bias and scale factor tests. By testing state-of-the-art gyroscopes, the effect of input rate stability and accuracy may be examined.

Based on the calculations of bias instability and ARW over the temperature range, there may be significant changes in gyroscope performance with temperature. The tests of one gyroscope showed a maximum 2.26°/h difference in bias instability and 0.012°/√h difference in ARW. This highlights the importance of the test procedure to characterize gyroscope performance with temperature and possibly create methods for calibration.

In the test of the PinPoint, the bias was not linear with temperature because of the integrated bias calibration feature. However, our test results could be used as a model to improve bias and scale factor calibration. Using the built-in calibration, the gyroscope could show up to 2.5°/s bias (based on manufacturer's 30-mV maximum bias variation).⁴ Using our results as a model, that bias could be reduced to 0.17°/s (1σ), an error reduction of 1/15. Similarly, scale factor calibration using our test results could reduce the 1% scale factor error to 0.1% (1σ).

Future tests with the LabVIEW setup may also determine whether gyroscopes have a temperature range at which they perform best. For the PinPoint tests there was a known operating range, but some state-of-the-art gyroscopes may be tested using this setup to determine the optimal operating temperatures.

5. Future Work

The test setup and procedure established by this project will be used to characterize gyroscopes, but before characterizing untested gyroscopes, the setup should be verified by testing state-of-the-art COTS gyroscopes. Further tests of gyroscopes with smaller error parameters, such as bias instability and ARW, will confirm that

the proposed tests can characterize new gyroscopes similarly. If the continued tests do not produce the expected results for the COTS gyroscopes, we may conclude that a more controlled setup is needed for state-of-the-art gyroscopes. Some suggestions for the controlled setup include the following:

- A smaller and more precise temperature chamber for less temperature fluctuation
- A thermocouple attached to the gyroscope to more accurately measure the temperature
- A filter to reduce noise provided by the power source
- A tumble test or bias analysis at a tilted position to remove the effect of Earth's rotation in the scale factor test
- A rate table with better rate stability and accuracy

Future additions to the test programs could include measurements of error values for scale factor and bias. Scale factor sensitivity, in parts per million per degrees Celsius, is defined by the maximum variation of the scale factor over a defined temperature range divided by that temperature range.¹ It could provide a direct comparison of how much a gyroscope's scale factor changes with temperature.

After the procedure is verified and/or altered, the test setup can be used to perform more than gyroscope characterization. In addition, it can be used to test methods of gyroscope performance improvement. For example, thermal mass could be added to the gyroscope to reduce its temperature fluctuation, or bias calibration can be tested after the bias sensitivity is determined from a preliminary test. The test procedure and LabVIEW programs will be useful for gyroscope characterization as well.

6. References

1. 647-2006 - IEEE standard specification format guide and test procedure for single-axis laser gyros. Piscataway (NJ): IEEE; 2006 Sep.
2. 1431-2004 - IEEE standard specification format guide and test procedure for coriolis vibratory gyros. Piscataway (NJ): IEEE; 2004 Dec.
3. Maio A, Smith G, Knight R, Nothwang W, Conroy J. Characterization of MEMS gyroscopes for navigation grade inertial measurement units. Adelphi (MD): Army Research Laboratory; Sep. 2014. Report No.: ARL-TR-7132.
4. PinPoint® CRM100 technical datasheet. Plymouth, Devon (UK): Silicon Sensing Systems Limited. 2013 Sep.
5. Sensors in Motion. MEMS symmetrical resonating gyroscope brief; Goleta (CA): 2014 Sep. [accessed 2016 June 24].
<http://www.sensorsinmotion.com/wp-content/uploads/2014/09/SensorsinMotionWhitePaper.pdf>.
6. Landmark 40 IMU datasheet. Snoqualmie (WA): Gladiator Technologies Division, LKD Aerospace, Inc.; 2015 Feb.
7. ButterflyGyro STIM210 datasheet. Horten (Norway): Sensoror AS; 2015 Apr.
8. Trusov A. Gyroscopes. In: Bhushan B, editor. Encyclopedia of nanotechnology. Netherlands: Springer; 2012. p. 1008–1020.
9. One-axis motion simulator model AC117 datasheet. Pittsburgh (PA): ACUTRONIC; 2016.

INTENTIONALLY LEFT BLANK.

Appendix. Angle Random Walk (ARW) Data

Table A-1 ARW over temperature as calculated by LabVIEW (1-s approximation) and Matlab (best fit), Trial 1

Temp	ARW1		ARW2		ARW3	
	LabVIEW	Matlab	LabVIEW	Matlab	LabVIEW	Matlab
-40	0.184134	0.14328	0.229201	0.17127	0.192414	0.15985
-15	0.190413	0.14533	0.240528	0.16122	0.198690	0.16096
10	0.180405	0.14551	0.200556	0.15713	0.188908	0.16951
25	0.175232	0.16237	0.192375	0.1631	0.185067	0.17524
35	0.175631	0.1653	0.194318	0.17789	0.186031	0.17861
60	0.176373	0.1651	0.190523	0.17556	0.190925	0.18482
85	0.184257	0.16461	0.201342	0.17107	0.216784	0.18357

Table A-2 ARW over temperature as calculated by LabVIEW (1-s approximation) and Matlab (best fit), Trial 2

Temp	ARW1		ARW2		ARW3	
	LabVIEW	Matlab	LabVIEW	Matlab	LabVIEW	Matlab
-40	0.187120	0.18731	0.232535	0.22788	0.207844	0.16557
-15	0.187481	0.14834	0.239231	0.16179	0.209181	0.16815
10	0.184494	0.15537	0.207369	0.16665	0.211668	0.19354
25	0.177727	0.16473	0.196495	0.1626	0.193065	0.18714
35	0.177050	0.16714	0.192446	0.16435	0.184594	0.18037
60	0.178964	0.17494	0.190565	0.18503	0.192529	0.19063
85	0.182785	0.15954	0.198293	0.19829	0.207134	0.17936

List of Symbols, Abbreviations, and Acronyms

ARW	angle random walk
COTS	commercial off-the-shelf
DAQ	data acquisition
DC	direct current
GPS	global positioning system
IMU	inertial measurement unit
MEMS	microelectromechanical systems
PNT	positioning, navigation, and timing
ppm	parts per million
rms	root-mean-square

1 DEFENSE TECHNICAL
(PDF) INFORMATION CTR
DTIC OCA

2 DIRECTOR
(PDF) US ARMY RESEARCH LAB
RDRL CIO L
IMAL HRA MAIL & RECORDS
MGMT

1 GOVT PRINTG OFC
(PDF) A MALHOTRA

7 US ARMY RSRCH LAB
(PDF) RDRL DE
GL SMITH
RDRL SE SEDD
K KAPPRA
RDRL SER L
B PIEKARSKI
J CONROY
R KNIGHT
W NOTHWANG
A MAIO